

# UNCLASSIFIED

AD NUMBER
AD018117
NEW LIMITATION CHANGE
TO Approved for public release, distribution unlimited
FROM Distribution authorized to U.S. Gov't. agencies and their contractors; Administrative/Operational Use; Aug 1953. Other requests shall be referred to Director, Wright Air Development Center, Wright-Patterson AFB, OH 45433.
AUTHORITY
AFAL ltr, 17 Aug 1979

THIS PAGE IS UNCLASSIFIED

WADC TECHNICAL REPORT 53-181

AD0018117 \*

FATIGUE PROPERTIES OF EXTRUDED MAGNESIUM ALLOY ZK 60  
UNDER VARIOUS COMBINATIONS OF ALTERNATING  
AND MEAN AXIAL STRESSES

A. A. BLATHERWICK  
and  
B. J. LAZAN

UNIVERSITY OF MINNESOTA

AUGUST 1953

Statement A  
Approved for Public Release

WRIGHT AIR DEVELOPMENT CENTER

20030708001

AD-018117

## NOTICES

When Government drawings, specifications, or other data are used for any purpose other than in connection with a definitely related Government procurement operation, the United States Government thereby incurs no responsibility nor any obligation whatsoever; and the fact that the Government may have formulated, furnished, or in any way supplied the said drawings, specifications, or other data, is not to be regarded by implication or otherwise as in any manner licensing the holder or any other person or corporation, or conveying any rights or permission to manufacture, use, or sell any patented invention that may in any way be related thereto.

The information furnished herewith is made available for study upon the understanding that the Government's proprietary interests in and relating thereto shall not be impaired. It is desired that the Judge Advocate (WCJ), Wright Air Development Center, Wright-Patterson Air Force Base, Ohio, be promptly notified of any apparent conflict between the Government's proprietary interests and those of others.

FATIGUE PROPERTIES OF EXTRUDED MAGNESIUM ALLOY ZK 60  
UNDER VARIOUS COMBINATIONS OF ALTERNATING  
AND MEAN AXIAL STRESSES

A. A. Blatherwick  
and  
B. J. Lazan

University of Minnesota

August 1953

Materials Laboratory  
Contract No. AF 33(038)-20840  
RDO No. 614-16

Wright Air Development Center  
Air Research and Development Command  
United States Air Force  
Wright-Patterson Air Force Base, Ohio

## FOREWORD

This report was prepared by the University of Minnesota, under USAF Contract No. AF 33(038)-20840. The contract was initiated under Research and Development Order No. 614-16, "Fatigue Properties of Structural Materials," and was administered under the direction of the Materials Laboratory, Directorate of Research, Wright Air Development Center, with Capt. R. A. Tondreau acting as project engineer.

In addition to the authors, the following personnel of the University of Minnesota contributed to this work: F. W. DeMoney, Metallurgist and H. Binder and P. M. Kemmer, Technicians.

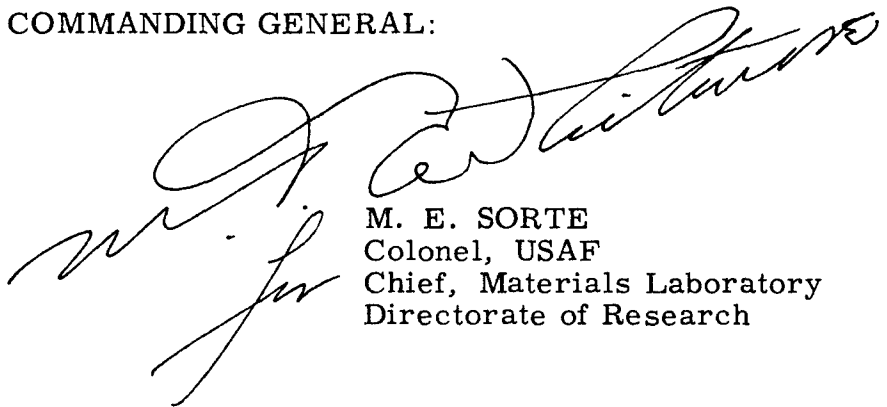
## ABSTRACT

Axial-stress fatigue tests were conducted on specimens of extruded magnesium alloy ZK60A-T5 under five selected ratios of alternating to mean stress. The data thus obtained are presented in the form of S-N diagrams, one curve for each stress ratio. The effects of varying the combinations of alternating and mean stresses are demonstrated by a series of stress-range diagrams. Three types of specimens (one unnotched and two notched) provide data for analysis of the fatigue strength reduction due to stress concentration. These data are illustrated by two types of charts showing the fatigue strength-reduction factor as a function of stress ratio, life, and stress magnitude.

## PUBLICATION REVIEW

This report has been reviewed and is approved.

FOR THE COMMANDING GENERAL:

A large, stylized handwritten signature in black ink, likely belonging to M. E. Sorte, is written over the printed name and title.

M. E. SORTE  
Colonel, USAF  
Chief, Materials Laboratory  
Directorate of Research

## TABLE OF CONTENTS

<u>Section</u>		<u>Page</u>
I	Introduction . . . . .	1
II	Test Program . . . . .	1
III	Material . . . . .	2
	3.1 Processing . . . . .	2
	3.2 Chemical Analysis . . . . .	2
	3.3 Metallographic Structure . . . . .	2
IV	Test Specimens . . . . .	3
	4.1 Design of Specimens . . . . .	3
	4.2 Preparation of Specimens . . . . .	3
V	Testing Equipment . . . . .	4
	5.1 Fatigue Testing Machines . . . . .	4
	5.2 Calibration . . . . .	4
VI	Results and Discussion . . . . .	5
	6.1 Static Tensile and Hardness Properties . . . . .	5
	6.2 Fatigue Properties . . . . .	5
VII	Summary and Conclusions . . . . .	8
	Bibliography . . . . .	11

## LIST OF TABLES

<u>Table</u>		
I	Static Properties of Magnesium, ZK 60A - T5 . . . . .	12
II	Fatigue Data on Type V Specimens ( $K_t = 1.0$ ) of Extruded Magnesium ZK 60A - T5 . . . . .	13
III	Fatigue Data on Type AB Specimens ( $K_t = 2.4$ ) of Extruded Magnesium ZK 60A - T5 . . . . .	14
IV	Fatigue Data on Type X Specimens ( $K_t = 3.4$ ) of Extruded Magnesium ZK 60A - T5 . . . . .	15

## LIST OF ILLUSTRATIONS

<u>Figure</u>		
1	Typical Microstructure of Magnesium Extrusion Alloy ZK 60A - T5 . . . . .	16
2	Fatigue Specimens, Types V, AB, and X . . . . .	17
3	S-N Fatigue Diagrams at Various Stress Ratios for Type V Specimens ( $K_t = 1.0$ ) of Extruded Magnesium Alloy ZK60 . . . . .	18
4	S-N Fatigue Diagrams at Various Stress Ratios for Type AB Specimens ( $K_t = 2.4$ ) of Extruded Magnesium Alloy ZK60 . . . . .	19
5	S-N Fatigue Diagrams at Various Stress Ratios for Type X Specimens ( $K_t = 3.4$ ) of Extruded Magnesium Alloy ZK60 . . . . .	20

# LIST OF ILLUSTRATIONS (cont.)

<u>Figure</u>		<u>Page</u>
6	Stress-Range Fatigue Diagrams for Type V Specimens ( $K_t = 1.0$ ) of Extruded Magnesium Alloy ZK60 . . . . .	21
7	Stress-Range Fatigue Diagrams for Type AB Specimens ( $K_t = 2.4$ ) of Extruded Magnesium Alloy ZK60 . . . . .	22
8	Stress-Range Fatigue Diagrams for Type X Specimens ( $K_t = 3.4$ ) of Extruded Magnesium Alloy ZK60 . . . . .	23
9	Fatigue Strength-Reduction "Contour" Curves for $K_t = 2.4$ Specimens of Extruded Magnesium Alloy ZK 60A - T5 Showing $K_f$ as a Function of N and Stress Ratio . . . . .	24
10	Fatigue Strength-Reduction "Contour" Curves for $K_t = 3.4$ Specimens of Extruded Magnesium Alloy ZK 60A - T5 Showing $K_f$ as a Function of N and Stress Ratio . . . . .	25
11	Fatigue Strength-Reduction "Contour" Curves for $K_t = 2.4$ Specimens of Extruded Magnesium Alloy ZK 60A - T5 Showing $K_f$ as a Function of $S_a$ and $S_m$ of the Unnotched Specimens . . . . .	26
12	Fatigue Strength-Reduction "Contour" Curves for $K_t = 3.4$ Specimens of Extruded Magnesium Alloy ZK 60A - T5 Showing $K_f$ as a Function of $S_a$ and $S_m$ of the Unnotched Specimens . . . . .	27



## SECTION I. INTRODUCTION

With the development of improved methods of obtaining magnesium, and especially the perfection of processes for extracting it from inexhaustible sea water, the use of magnesium alloys in engineering has become very important. Its advantages of lightness, machinability, and durability make it especially desirable for use in aircraft as well as in other machines and structures where weight reduction is essential. Certainly, vast increase may be expected in the use of this material. However, before it can be extensively used, additional data must be obtained on which design can be based.

The work undertaken in this program provides some fatigue data on extruded magnesium alloy ZK60A-T5 under various combinations of mean and alternating axial stresses. The effects of stress concentration due to notches are analyzed, and diagrams are included which should be of some help to the designer faced with the ever-present problem of stress raisers in the form of holes, notches, and fillets.

## SECTION II. TEST PROGRAM

All fatigue tests in this work were made under axial stress, the ratio of alternating to mean stress,  $A$ , being varied so as to provide data for investigating the effect of stress range on fatigue life. The stress ratios,  $A$ , used were infinity (completely reversed stress), 1.4, 0.6, 0.25, and 0 (static stress). In a few tests a stress ratio of 0.1 was used to provide more complete data in the range of relatively low alternating stress. Sufficient data were obtained at each stress ratio to establish an S-N curve in the range from  $5 \times 10^3$  to  $2 \times 10^7$  cycles.

Three types of specimens were employed, one of which was un-notched while the other two were notched. Each of the specimen types was tested at all stress ratios, thus data were obtained from which an analysis of notch sensitivity could be made. A more detailed description of specimens is given in Section IV.

## SECTION III. MATERIAL

### 3.1 Processing

The material tested in this program was magnesium alloy ZK60A-T5 in extruded bar stock form as furnished by The Dow Chemical Company.

All the bars were  $1\frac{1}{4}$  in. in diameter and were cut to 10 ft. lengths.<sup>1</sup> They were extruded from three billets from the center of the batch at a temperature of 625° to 680° F and at a push rate of 5 to 7 ft. per minute. They were artificially aged at 300° F for 24 hours.

### 3.2 Chemical Analysis

The spectographic analysis of this material, as furnished by The Dow Chemical Company is as follows: <.002% Al, <.0002% Ba, <.015% Ca, <.01% Cu, <.001% Fe, <.04% Mn, <.001% Ni, <.005% Pb, <.05% Si, 5.6% Zn, and .66% Zr.

### 3.3 Metallographic Structure

The typical microstructure of this material is shown in Figure 1. This alloy is a solid solution precipitation hardening type with the Mg-Zn compound as the submicroscopic precipitate. The alpha Mg solid solution containing substitutional elements magnesium and zirconium constitute the structure of this alloy. From the transverse micrographs it may appear that this is a two-phase alloy, having an island constituent in a matrix material. However, this is believed due to the orientation of the various solid solution single phase grains formed and distorted in the extrusion process. Thus, some grains are favorably oriented with respect to the incident illumination and appear as isolated grains, whereas others not so oriented lose their identity. The directional orientation of the grains due to the extrusion process is clearly seen in the micrographs taken of the longitudinal section.

---

<sup>1/</sup> Bars were carefully marked to identify their position in the original billet and their extrusion number in case it might become necessary to try to associate excessive scatter in the data with material inhomogeneities. The results did not necessitate this procedure, however.

The structure of this alloy appears fairly uniform in the bars examined and quite free from inclusions. Only a few inclusions, probably of manganese, were visible in each field of view.

## SECTION IV. TEST SPECIMENS

### 4.1 Design of Specimens

The three types of specimens used in this program, shown in Figure 2, have a minimum diameter of 0.400 in. at the test section. The single fillet produces insignificant stress concentration and thus the theoretical stress concentration factor,  $K_t$ , is taken as one for the unnotched type. The other two types have the same shape, except that at the root of the fillet there is a circumferential 60° V notch. One type has a root radius of 0.032 in. and the second has a root radius of 0.010 in. The  $K_t$  values of 2.4 and 3.4 shown for these notched specimens were computed from Neuber's charts (1)<sup>1</sup>.

### 4.2 Preparation of Specimens

Careful attention was given to the procedures in preparing the specimens to avoid as far as practicable the possibility of residual stress and cold working due to machining. Tool bits were kept sharp and coolants were used during the rough turning. Progressively shallower cuts were taken during the finish turning, 0.005 in. being removed on the last pass, leaving the specimen 0.015 in. oversize.

The unnotched specimen was then finished in three polishing steps by a belt sander under controlled pressure (2). The first step removed 0.012 in. in six passes with a 240 grit aluminum oxide belt, while the second step removed 0.002 in. with a 400 grit belt leaving circumferential scratches. In the third step, the direction of rotation was reversed and speeds so adjusted that scratches were longitudinal. This step removed all circumferential scratches. Kerosene was used as a lubricant in the polishing operation and the surface produced was better than 10 micro-inches.

---

<sup>1</sup>/ Numbers in parenthesis are references to the Bibliography

The fillets of the notched specimens were turned and then the notches were ground using an aluminum oxide wheel No. A80-M600, dressed to the required shape, and lubricated with a sulfur cutting oil.

The sharp-notch specimens were given no further treatment. The moderate-notch specimens however, were lapped, using a copper rod and 600 grit alundum lapping compound to remove the circumferential grinding scratches. Further details are given in reference (3).

The test sections of all specimens were protected from corrosion by wrapping them in wax tape immediately after final preparation.

## SECTION V. TESTING EQUIPMENT

### 5.1 Fatigue Testing Machines

All fatigue tests were conducted in axial-stress machines capable of imposing on the specimen any force combination up to

5000 pounds alternating force and 9000 pounds static tensile force. The alternating force is produced by a rotating eccentric driven by a 3600 rpm synchronous motor. The static force is applied by means of calibrated helical springs so controlled that the force is maintained constant even if the specimen elongates during a test. Specially designed gripping devices are used to eliminate as far as possible bending stresses due to gripping the specimen. A detailed description of test equipment is given in reference (3).

### 5.2 Calibration

Considerable care was taken to insure that the stresses imposed during the tests were accurately controlled. Machines were originally calibrated by three independent methods and spot checks were made throughout the test program. Average stress and stress distribution were thus maintained to within  $\pm 5$  percent of desired values at all times.

## SECTION VI. RESULTS AND DISCUSSION

### 6.1 Static Tensile and Hardness Properties

In order to evaluate the uniformity of the test material from bar to bar and to compare its static strengths with published values, (4), (5), (6), static tensile and hardness tests were performed. Specimens were prepared from blanks taken from one end of each 10 ft. bar, and standard ASTM tests were conducted to determine tensile strength, yield strength, modulus of elasticity, and percent elongation. These values, together with Rockwell A hardness data are given in Table I. The tensile and yield strengths compare quite favorably with accepted values, but the elongation is considerably higher than that listed by The Dow Chemical (4) for this material.

Tensile tests were also performed on two specimens of each fatigue type to determine the static ultimate strength. It will be observed that the tensile strength of the filleted specimen is significantly higher than that of the ASTM specimen and that the notched specimens display still higher tensile strengths. This effect is in agreement with previous observations (3) and (6).

### 6.2 Fatigue Properties

The fatigue data obtained on the three types of specimens are listed in Tables II, III, and IV. These data are plotted and analyzed by means of the diagrams described below.

6.2.1 S-N Diagrams. S-N diagrams are shown in Figures 3, 4, and 5 for the unnotched specimens and for the intermediate and sharp-notch specimens respectively. In each of these diagrams the logarithm of the crest stress (maximum stress during a cycle) is plotted against the logarithm of the number of cycles to failure; one curve representing each test stress ratio. The logarithmic scale was used for the ordinates because it produces better separation of the curves at low stress, and because a fixed distance represents a constant percentage at any ordinate. A 10 percent spread is indicated on the diagrams for convenience.

In Figure 3, the curves for the unnotched specimens are quite flat in all cases with a rather abrupt knee at about  $10^5$  cycles. All of the curves appear to be nearly horizontal beyond this point indicating a definite endurance limit, though more data should be obtained to demonstrate this observation conclusively.

As is expected the curve for reversed stress ( $A = \infty$ ) shows the lowest fatigue strength, while decreasing the relative amount of alternating stress increases the fatigue strength based on maximum stress during the cycle. It may be noted that some specimens were tested at a maximum stress in excess of the static ultimate strength and yet they did not fail in as many as 40,000 cycles. This observation is in agreement with others previously reported (3), (6), and although an investigation of this behavior is beyond the scope of this report, it may be partially explained on the basis of: (a) the very short period of time in each cycle during which the stress exceeds the static ultimate strength, (b) the effect of strain rate, (c) the strengthening of the material by strain hardening, and (d) the magnitude of imposed stresses during very short-term tests which may not be as high as calibrations indicate because of rapid elongation of the specimen and resultant temporary reduction in pre-stress. However, for tests in excess of 2000 cycles, the automatic preload control mechanism functions rapidly enough to maintain the desired static force.

The curves for the intermediate-notch specimens and for the sharp-notch specimens shown in Figures 4 and 5 respectively, are lower and steeper as should be expected, since the static strengths of these specimens are higher than that of the unnotched specimens. Within the range of data procured, these curves do not become horizontal, thus no definite endurance limit may be given.

**6.2.2 Stress Range Diagrams.** Figures 6, 7, and 8 are presented to clarify the effect on fatigue strength of varying the relative magnitudes of alternating and mean stress. These curves show combinations of alternating and mean stress that may be endured for a given life. The radial lines through the origin represent the test stress ratios (the vertical axis being  $A = \infty$  and the horizontal axis representing static tests). Thus all plotted points, taken from the corresponding S-N curves, must fall on these lines. The dashed line extending from the point on the horizontal axis corresponding to the static ultimate strength upward at a  $45^\circ$  angle represents combinations of stress equal to the static ultimate strength.

In Figure 6 the constant-life curves for unnotched specimens are shown. The curve for a life of  $10^7$  cycles is practically a straight line from the fatigue strength under reversed stress ( $A = \infty$ ) to the static

ultimate strength. If the slope of this line were 1 (45° angle with axis) the relative effect of alternating and mean stress would be the same. However, since the slope is flatter, the effect on fatigue life of varying the mean stress is not as critical as that of varying alternating stress.

This behavior is much more pronounced in the case of the notched specimens shown in Figures 7 and 8 where the curves for  $10^5$  and  $10^7$  cycles for both specimen types are very flat. These diagrams show clearly that notched specimens are very sensitive to alternating stress and that even a small vibration may seriously reduce the allowable crest stress that may be imposed.

These diagrams indicate again that, since the experimental curves sometimes lie above the  $S_a + S_m = S_u$  line for short life tests and at low stress ratio, the maximum stress may exceed the static ultimate strength.

6.2.3 Notch Sensitivity. To analyze the effect of a notch or other stress raiser on the fatigue strength of the material, the fatigue strength reduction factor is defined as follows:

$$K_f = \frac{S_c \text{ (unnotched specimen)}}{S_c \text{ (notched specimen)}} \text{ for a given life. }^1$$

The diagrams of Figures 9 and 10 show the behavior of  $K_f$  as a function of life and of stress ratio. These "contour" curves were developed by first plotting a set of "profile" curves (one for each stress ratio) of  $K_f$  versus life and another set of profiles of  $K_f$  versus  $R^2$  for each of several values of  $N$ . Selected values of  $K_f$  were then projected onto the corresponding stress-ratio or life line to establish points (not shown) in the grids of Figures 9 and 10. The contour curves were then drawn so as to connect points of equal value.

---

<sup>1/</sup> In an analysis based on fixed stress ratio, the ratios of crest stress, alternating stress, and mean stress are all the same.

<sup>2/</sup>  $R$  is the ratio of minimum stress in a cycle ( $S_t$ ) to the crest stress ( $S_c$ ) and is used in these diagrams because its range from -1.0 to 1.0 is more convenient to plot than the range of  $A$  from 0 to  $\infty$ .

Several observations may be made from a study of Figures 9 and 10. It is quite apparent that the maximum value of  $K_f$  occurs under reversed stress ( $A = \infty$ ) and at long life. The close-packed contours in the upper portion of the diagrams indicate that  $K_f$  falls off sharply as the relative amount of alternating stress is reduced. In this region  $K_f$  is relatively independent of life but is very sensitive to stress ratio. In the lower half of the diagrams,  $K_f$  is affected more by life and is not so critically dependent on stress ratio. Maximum observed values of  $K_f$  are 2.2 for type AB specimens ( $K_t = 2.4$ ) and 2.9 for type X specimens ( $K_t = 3.4$ ).

In Figures 11 and 12,  $K_f$  is shown as a function of stress ratio and stress magnitude by means of contours of constant  $K_f$  plotted on a grid of alternating versus mean stress in the unnotched specimen. These curves were developed by first plotting "profile" curves (not shown) of  $K_f$  versus either  $S_a$  or  $S_m$ , and then the desired  $K_f$  values were located on the radial stress-ratio lines of Figures 11 and 12. The points thus located (not shown in the figures) were then connected by the contour curves. The sloping dashed line represents the stress combinations in the unnotched specimen resulting in a life of  $10^7$  cycles. Since the S-N curves are practically horizontal at this life, no points can be plotted for stresses below this line which forms a terminus for the contour curves.

In these figures, the effect of stress magnitude on the fatigue strength-reduction factor is readily observed. At all stress ratios,  $K_f$  drops off sharply as the stress is increased. Here again, it may be seen that  $K_f$  is maximum at  $A = \infty$  and that at low stress ratios  $K_f$  has its lowest values. This should be expected, since  $K_f$  is less than 1 under static tests (the static ultimate strength of the notched specimens being larger than that of the unnotched specimens).

## SECTION VII. SUMMARY AND CONCLUSIONS

A series of axial-stress fatigue tests at room temperature were conducted on specimens of extruded magnesium alloy ZK60A-T5.



Tests were run at stress ratios,  $A^1$ , of  $\infty$ , 1.4, 0.6, 0.25, and 0 on each of three specimen types, one of which was unnotched, while the other two were notched. Standard static tension and hardness tests were also performed to provide a basis for comparison of the test material with generally accepted standards.

The results of the fatigue tests were presented primarily in the form of S-N diagrams, one curve for each stress ratio and specimen type (Figures 3, 4, and 5). A comparison of the stress-ratio curves for a given specimen type provided information on the effect of stress range on fatigue life. This effect was illustrated by means of the stress range diagrams given in Figures 6, 7, and 8.

The effect of stress concentration produced by a notch was examined by a comparison of the S-N curves, for a given stress ratio, for the notched and unnotched specimens. The fatigue strength reduction factor,  $K_f^2$ , was studied by means of diagrams showing its variation with stress ratio and life (Figures 9 and 10) and with stress ratio and stress level (Figures 11 and 12).

The following are conclusions reached through the analysis of data obtained in this program:

- (a) The S-N curves for unnotched specimens became very flat beyond  $10^5$  cycles, indicating the apparent existence of an endurance limit. However, this observation is not so definite for the mild-notch specimens and is even less pronounced for the sharp notch. If an endurance limit exists for the notched specimens, it must become evident at a life greater than  $2 \times 10^7$  cycles.
- (b) The flatness of the stress-range diagrams indicates that the fatigue life of this magnesium alloy is more sensitive to alternating stress than to mean stress. This is especially true for notched specimens at long life where the addition of

---

<sup>1/</sup>  $A$  is the ratio of the alternating stress,  $S_a$ , to the static mean stress,  $S_m$ .

<sup>2/</sup>  $K_f$  is defined as the ratio of the fatigue strength for a given life of the unnotched specimen to that of the notched specimen at the same life.

an alternating stress of 10% of the static ultimate strength will necessitate decreasing the allowable mean stress by as much as 80%.

- (c) The fatigue strength-reduction factor,  $K_f$ , varies with stress ratio and stress magnitude (or life). At low stress ratios,  $K_f$  is critically dependent on stress ratio, increasing sharply as the stress ratio increases, and is relatively independent of life (or stress level). However, at higher stress ratio,  $K_f$  is affected more by stress magnitude, and stress ratio is less important.

## BIBLIOGRAPHY

- (1) H. Neuber, "Theory of Notch Stresses," Edwards Brothers, Ann Arbor, Michigan, 1946.
- (2) B. J. Lazan and T. Wu, "Damping, Elasticity, and Dynamic Stress-Strain Properties of Mild Steel," Proc. ASTM, Vol. 51, (1951).
- (3) B. J. Lazan and A. A. Blatherwick, "Fatigue Properties of Aluminum Alloys at Various Direct Stress Ratios," WADC Technical Report 52-307, Part I, Wright Air Development Center, 1952.
- (4) The Dow Chemical Company, "Magnesium Alloys and Products," Midland, Michigan, 1950.
- (5) The Dow Chemical Company, "Fatigue Properties of Magnesium-Alloy Forgings," Seventeenth Interim Report to the Air Material Command, USAF, November 1952.
- (6) W. J. Trapp, "Mechanical Properties of Extruded Magnesium Alloys - ZK 60 and AZ 80," AF Technical Report No. 5926, Wright-Patterson Air Force Base, Ohio, 1950.

TABLE I. STATIC PROPERTIES OF MAGNESIUM, ZK 60A-T5

Specimen No. and Type *	Hardness $R_A$	Mod. E $10^6$ PSI	Tensile Strength PSI	.2% Offset Yield Str. PSI	Elong.
AD 1958 AE	27.7	6.13	46,000	39,100	20%/2"
AD 1959 AE	26.5	5.98	46,100	40,700	21%/2"
AD 1960 AE	27.5	6.15	46,100	40,000	22%/2"
AD 1961 AE	28.9	6.24	49,500	43,600	21%/2"
AD 1962 AE	28.5	6.19	46,600	39,500	22%/2"
AD 1963 AE	27.9	6.30	46,600	40,600	20%/2"
AD 1964 AE	29.0	5.92	47,400	42,900	24%/2"
AD 1965 AE	28.6	6.02	47,400	41,100	22%/2"
AD 1966 AE	28.1	6.15	48,900	41,000	20%/2"
AD 1967 AE	29.0	6.26	49,400	40,300	21%/2"
AD 1968 AE	28.5	6.42	48,300	41,100	22%/2"
AD 1969 AE	28.1	6.11	47,200	41,300	22%/2"
Average	28.2	6.15	47,500	40,900	21.4%/2"
<hr/>					
AD 2014 V			52,000		0.178"
AD 1998 V			51,500		0.183"
Average for Type V Specimens ( $K_t = 1.0$ )			51,800		0.180"
<hr/>					
AD 2034 AB			63,500		0.027"
AD 2055 AB			63,800		0.024"
Average for Type AB Specimens ( $K_t = 2.4$ )			63,700		0.025"
<hr/>					
AD 2102 X			58,700		0.035"
AD 2092 X			57,600		0.036"
Average for Type X Specimens ( $K_t = 3.4$ )			58,200		0.035"

\* Standard ASTM specimen and test.

TABLE II. FATIGUE DATA ON TYPE V SPECIMENS  
( $K_t = 1.0$ ) OF EXTRUDED MAGNESIUM ZK 60A - T5

Specimen Number	Stress Ratio A	Crest Stress KSI	Kilocycles to Failure
AD 1994 V	0.25	56.0	15.1
AD 1986 V	0.25	53.0	28.4
AD 1974 V	0.25	50.0	52.6
AD 1978 V	0.25	45.0	90.0
AD 1990 V	0.25	41.0	259.0
AD 1982 V	0.25	37.0	20,200.0 *
AD 1993 V	0.6	55.0	9.0
AD 1989 V	0.6	51.0	12.6
AD 1977 V	0.6	45.0	28.1
AD 1981 V	0.6	38.0	59.4
AD 1985 V	0.6	36.0	626.0
AD 1973 V	0.6	35.0	6,410.0
AD 1991 V	1.4	45.0	5.4
AD 1983 V	1.4	41.0	20.8
AD 1974 V	1.4	35.0	32.4
AD 1979 V	1.4	30.0	59.4
AD 1999 V	1.4	29.0	4,930.0
AD 1995 V	1.4	28.0	11,100.0 * B. T.
AD 1987 V	1.4	27.0	21,000.0 *
AD 1992 V	$\infty$	29.0	11.9
AD 2004 V	$\infty$	27.0	29.5
AD 1988 V	$\infty$	25.0	51.2
AD 1996 V	$\infty$	23.0	64.1
AD 2007 V	$\infty$	22.0	1,190.0
AD 1984 V	$\infty$	22.0	1,810.0 * B. T.
AD 2000 V	$\infty$	21.0	3,100.0 * B. T.
AD 2012 V	$\infty$	20.0	29,900.0 *

\* Did not fail.

B. T. Broke in threads.

TABLE III. FATIGUE DATA ON TYPE AB SPECIMENS  
( $K_t = 2.4$ ) OF EXTRUDED MAGNESIUM ZK 60A - T5

Specimen Number	Stress Ratio A	Crest Stress KSI	Kilocycles to Failure
AD 2058 AB	0.1	39.0	5,160.0 *
AD 2058 AB **	0.1	45.0	195.0
AD 2061 AB	0.1	60.0	17.1
AD 2043 AB	0.25	20.0	20,700.0 *
AD 2045 AB	0.25	22.0	20,300.0 *
AD 2052 AB	0.25	23.0	30,000.0 *
AD 2052 AB	0.25	23.0	20,400.0 *
AD 2031 AB	0.25	23.0	85.0
AD 2023 AB	0.25	25.0	140.0
AD 2035 AB	0.25	35.0	32.1
AD 2019 AB	0.25	45.0	14.4
AD 2039 AB	0.25	47.0	12.9
AD 2049 AB	0.25	57.0	5.03
AD 2044 AB	0.6	15.0	20,000.0 *
AD 2029 AB	0.6	16.0	767.0
AD 2040 AB	0.6	18.0	20,300.0 *
AD 2046 AB	0.6	19.0	20,100.0 *
AD 2024 AB	0.6	20.0	36.0
AD 2057 AB	0.6	20.0	79.3
AD 2051 AB	0.6	21.0	89.6
AD 2054 AB	0.6	23.0	31.8
AD 2032 AB	0.6	27.0	18.7
AD 2020 AB	0.6	35.0	7.56
AD 2036 AB	0.6	40.0	4.32
AD 2042 AB	1.4	13.0	19,400.0 *
AD 2028 AB	1.4	15.0	72.5
AD 2053 AB	1.4	17.5	28.1
AD 2025 AB	1.4	20.0	24.1
AD 2056 AB	1.4	22.0	16.2
AD 2059 AB	1.4	25.0	10.6
AD 2021 AB	1.4	25.0	2.63
AD 2033 AB	1.4	26.0	1.08
AD 2047 AB	$\infty$	9.0	24,600.0 *
AD 2041 AB	$\infty$	10.0	8,800.0
AD 2030 AB	$\infty$	11.0	540.0
AD 2022 AB	$\infty$	13.0	77.4
AD 2026 AB	$\infty$	14.6	29.5
AD 2038 AB	$\infty$	17.0	14.0
AD 2037 AB	$\infty$	19.0	1.08
AD 2060 AB	$\infty$	19.0	8.64

\* Did not fail.

\*\* Previous stress history.

TABLE IV. FATIGUE DATA ON TYPE X SPECIMENS  
( $K_t = 3.4$ ) OF EXTRUDED MAGNESIUM ZK 60A - T5

Specimen Number	Stress Ratio A	Crest Stress KSI	Kilocycles to Failure	
AD 2100 X	0.1	29.0	13,800.	*
AD 2100 X	0.1	31.5	6,550.	*
AD 2094 X	0.1	33.0	266.	
AD 2100 X	0.1	35.0	400.	
AD 2086 X	0.25	20.0	30,800.	*
AD 2082 X	0.25	21.0	313.	
AD 2091 X	0.25	21.5	324.	
AD 2078 X	0.25	23.0	389.	
AD 2074 X	0.25	26.0	136.	
AD 2066 X	0.25	31.0	90.4	
AD 2514 X	0.25	34.0	14.8	
AD 2513 X	0.25	35.0	18.7	
AD 2062 X	0.25	40.0	26.3	
AD 2070 X	0.25	46.0	5.58	
AD 2087 X	0.6	17.0	18,600.	
AD 2083 X	0.6	18.0	432.	
AD 2084 X	0.6	19.0	49.4	
AD 2079 X	0.6	20.0	122.	
AD 2075 X	0.6	23.0	23.6	
AD 2071 X	0.6	25.0	16.7	
AD 2067 X	0.6	32.0	3.96	
AD 2063 X	0.6	42.0	1.26	
AD 2095 X	1.4	12.0	23,600.	*
AD 2080 X	1.4	13.0	11,100.	
AD 2099 X	1.4	14.0	83.9	
AD 2076 X	1.4	15.0	79.5	
AD 2072 X	1.4	17.0	51.5	
AD 2068 X	1.4	21.0	8.64	
AD 2064 X	1.4	25.0	4.68	
AD 2104 X	$\infty$	7.40	24,100.	*
AD 2101 X	$\infty$	8.00	4,430.	
AD 2097 X	$\infty$	8.00	1,190.	
AD 2093 X	$\infty$	8.50	2,090.	
AD 2089 X	$\infty$	9.50	270.	
AD 2088 X	$\infty$	10.0	130.	
AD 2085 X	$\infty$	10.0	187.	
AD 2077 X	$\infty$	11.0	218.	
AD 2073 X	$\infty$	13.0	25.6	
AD 2069 X	$\infty$	15.0	14.8	
AD 2065 X	$\infty$	18.0	5.58	
AD 2081 X	$\infty$	21.0	3.60	

\* Did not fail.

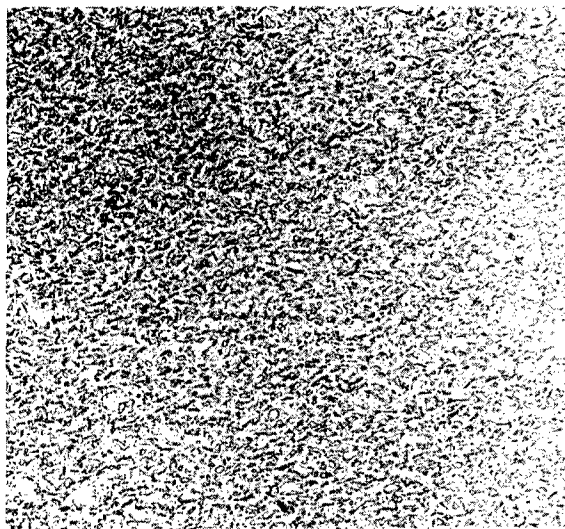


75X



250X

### LONGITUDINAL SECTION



75X



250X

### TRANSVERSE SECTION

Etchant:- 1 Part  $\text{HNO}_3$ ; 24 Parts  $\text{H}_2\text{O}$ ; 75 Parts Glycol

FIG. 1 TYPICAL MICROSTRUCTURE OF MAGNESIUM  
EXTRUSION ALLOY ZK 60A - T5



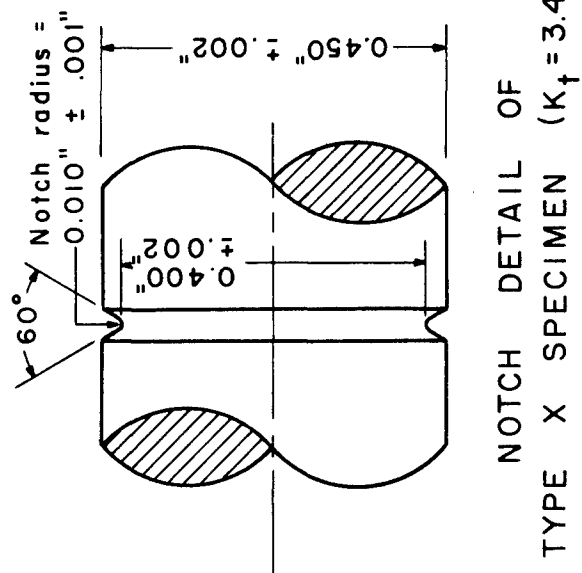
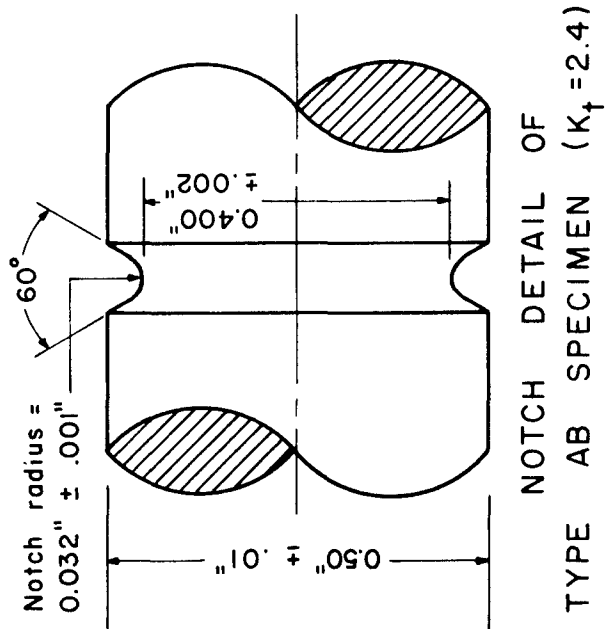
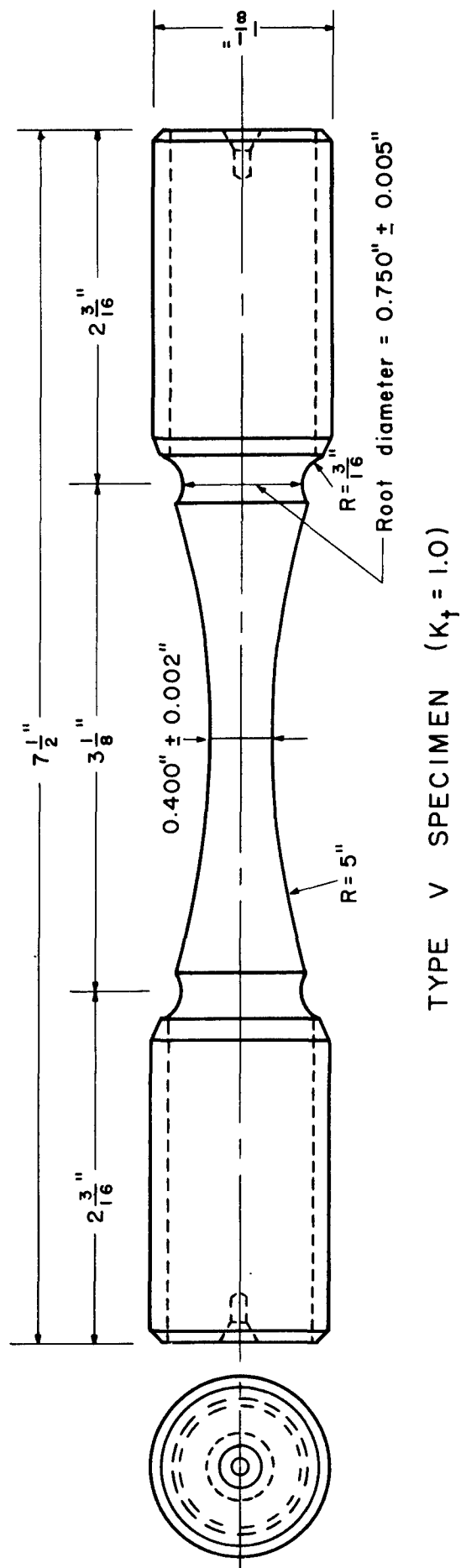


FIG. 2 FATIGUE SPECIMENS, TYPES V, AB, AND X

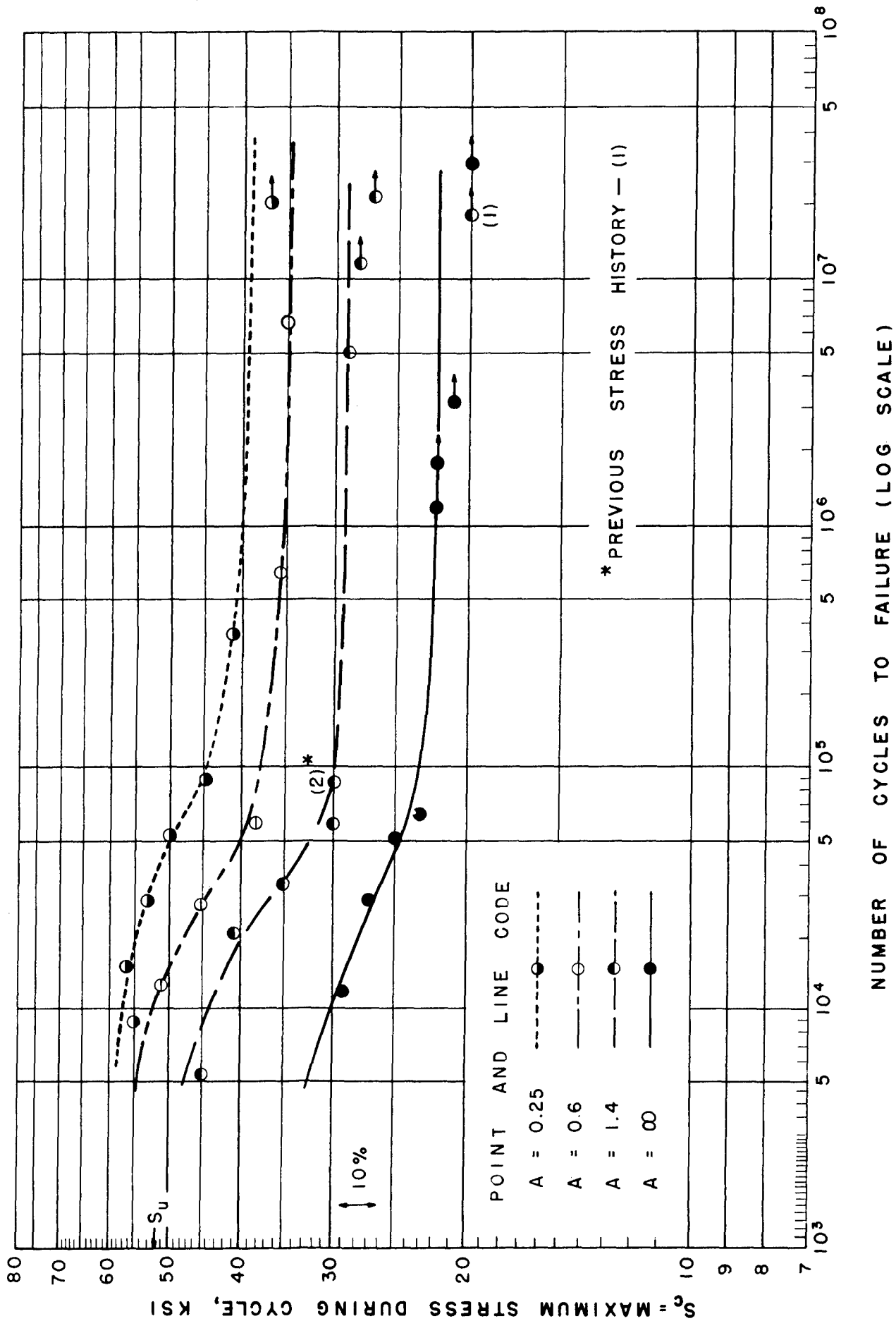


FIG. 3 S-N FATIGUE DIAGRAMS AT VARIOUS STRESS RATIOS FOR

TYPE V SPECIMENS ( $K_t = 1.0$ ) OF EXTRUDED MAGNESIUM ALLOY ZK60

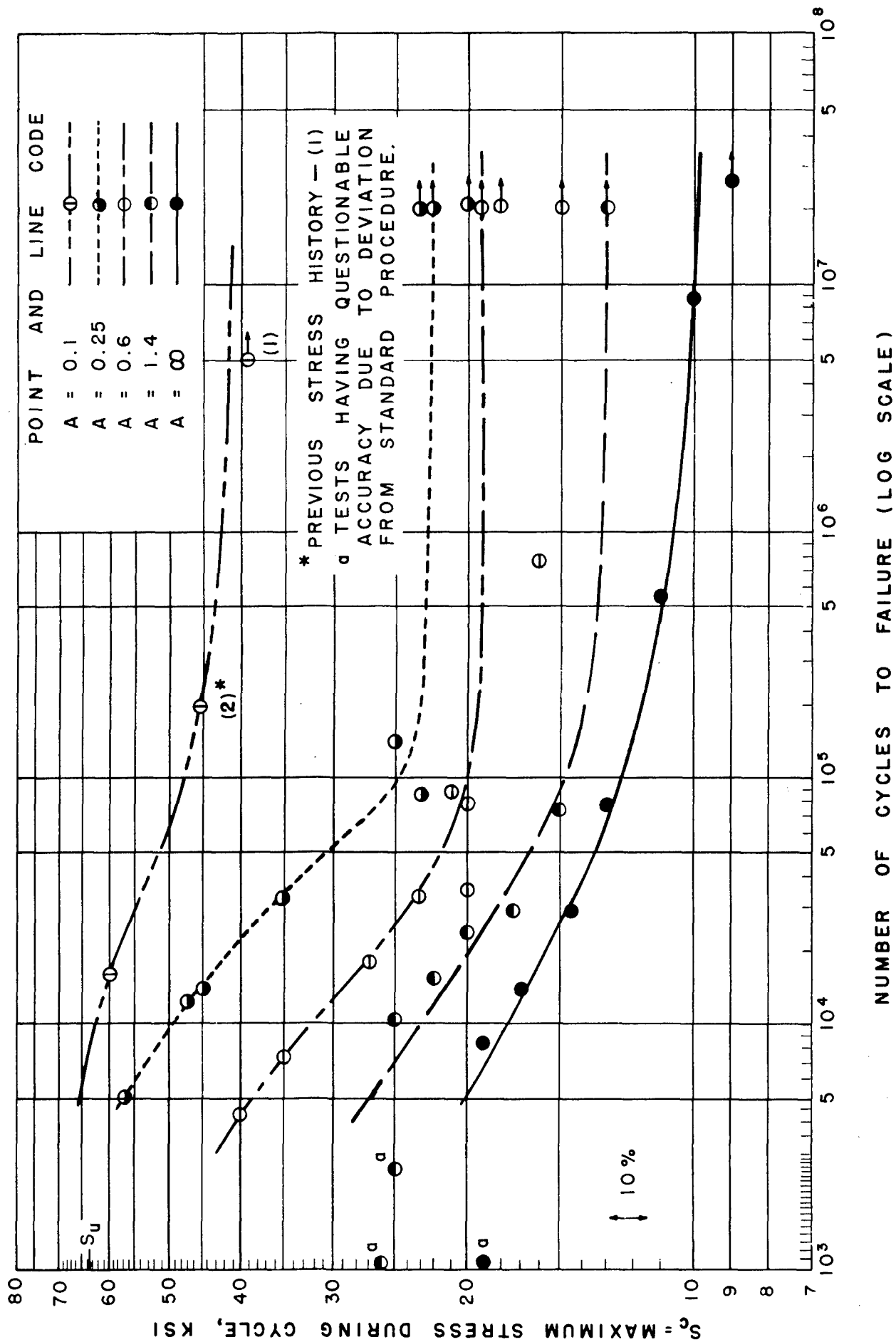


FIG. 4 S-N FATIGUE DIAGRAMS AT VARIOUS STRESS RATIOS FOR TYPE AB SPECIMENS ( $K_t = 2.4$ ) OF EXTRUDED MAGNESIUM ALLOY ZK60

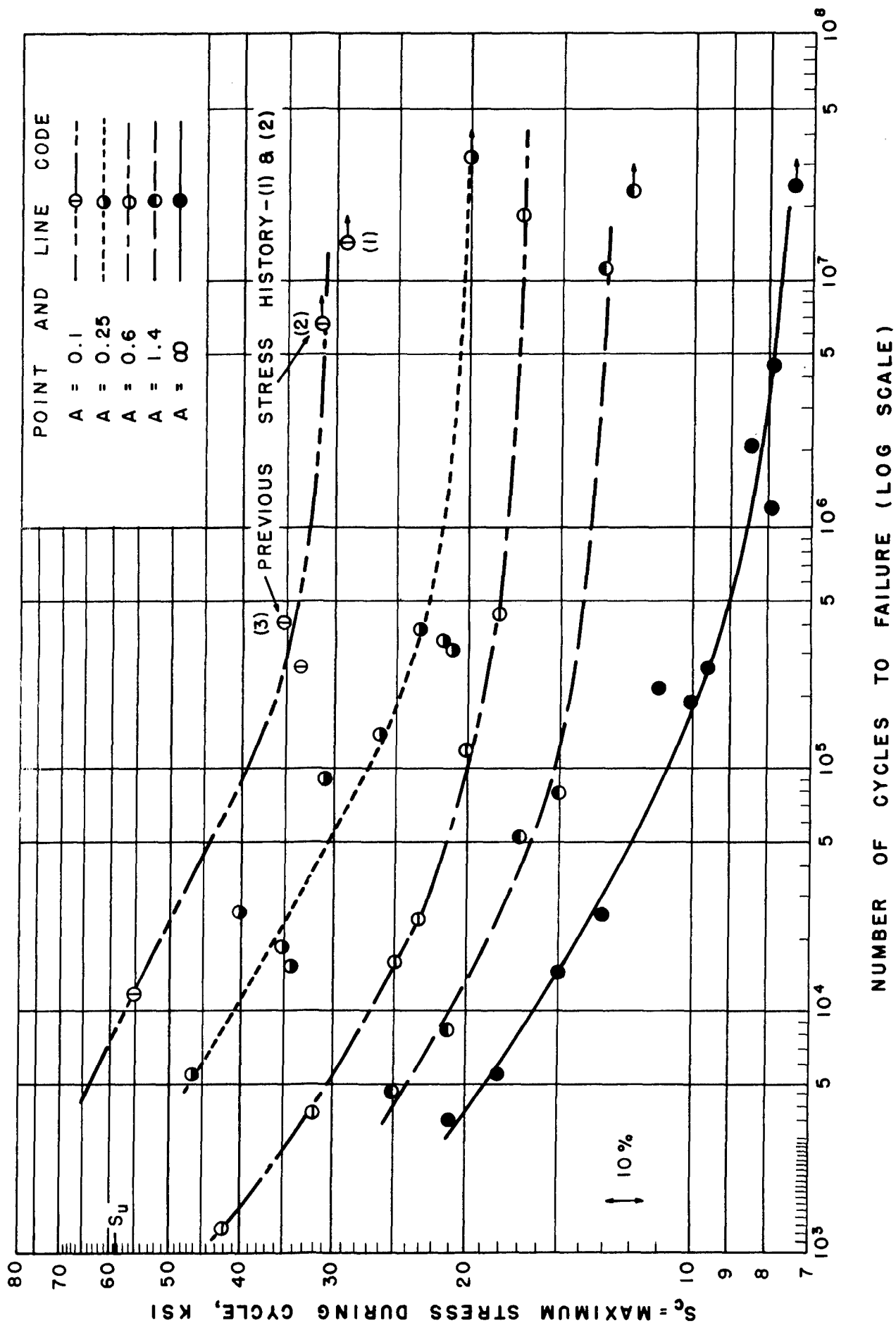


FIG. 5 S-N FATIGUE DIAGRAMS AT VARIOUS STRESS RATIOS FOR TYPE X SPECIMENS ( $K_t = 3.4$ ) OF EXTRUDED MAGNESIUM ALLOY ZK60

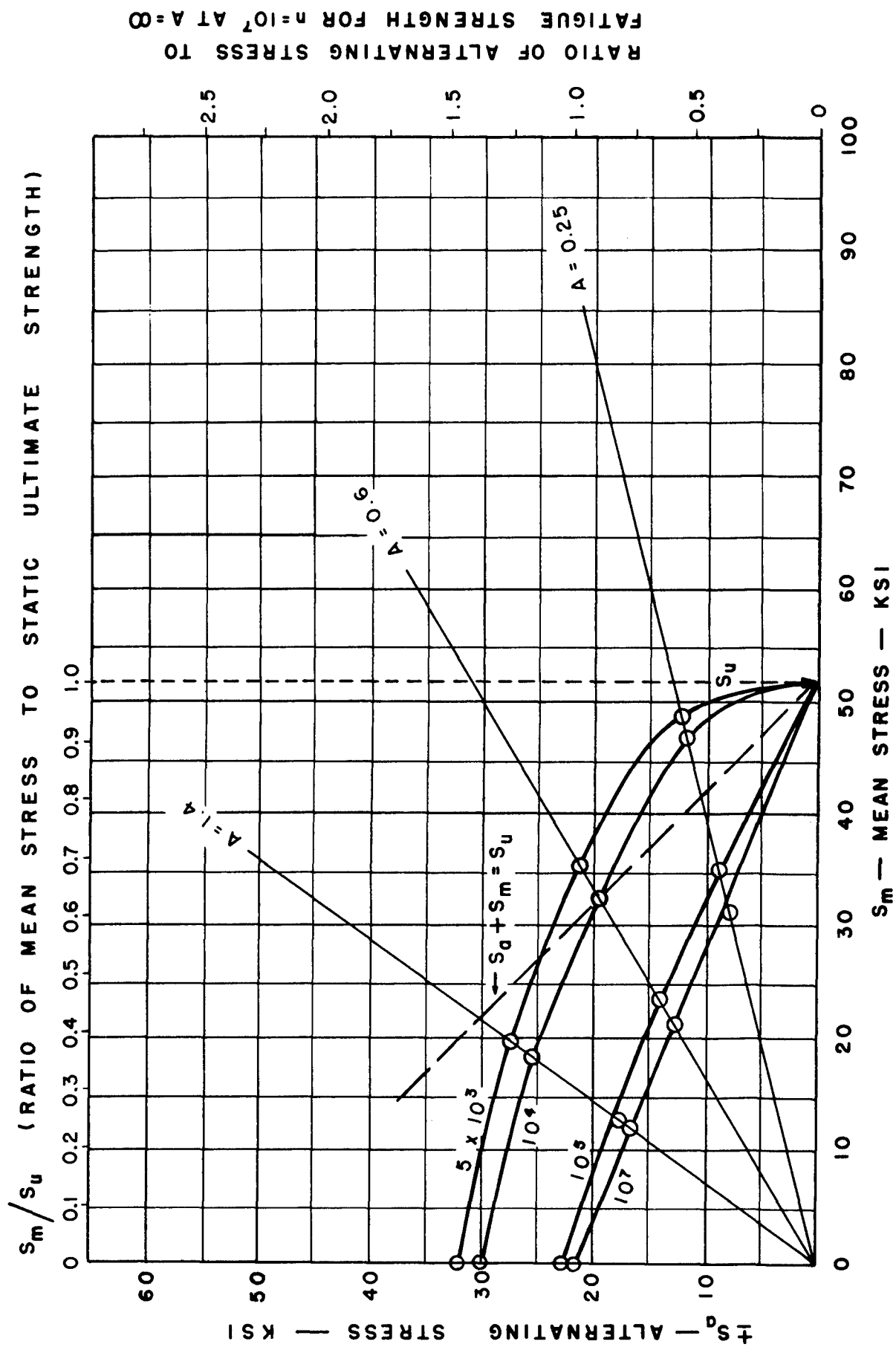


FIG. 6 STRESS-RANGE FATIGUE DIAGRAMS FOR  
TYPE V SPECIMENS ( $K_t = 1.0$ ) OF EXTRUDED MAGNESIUM ALLOY ZK60

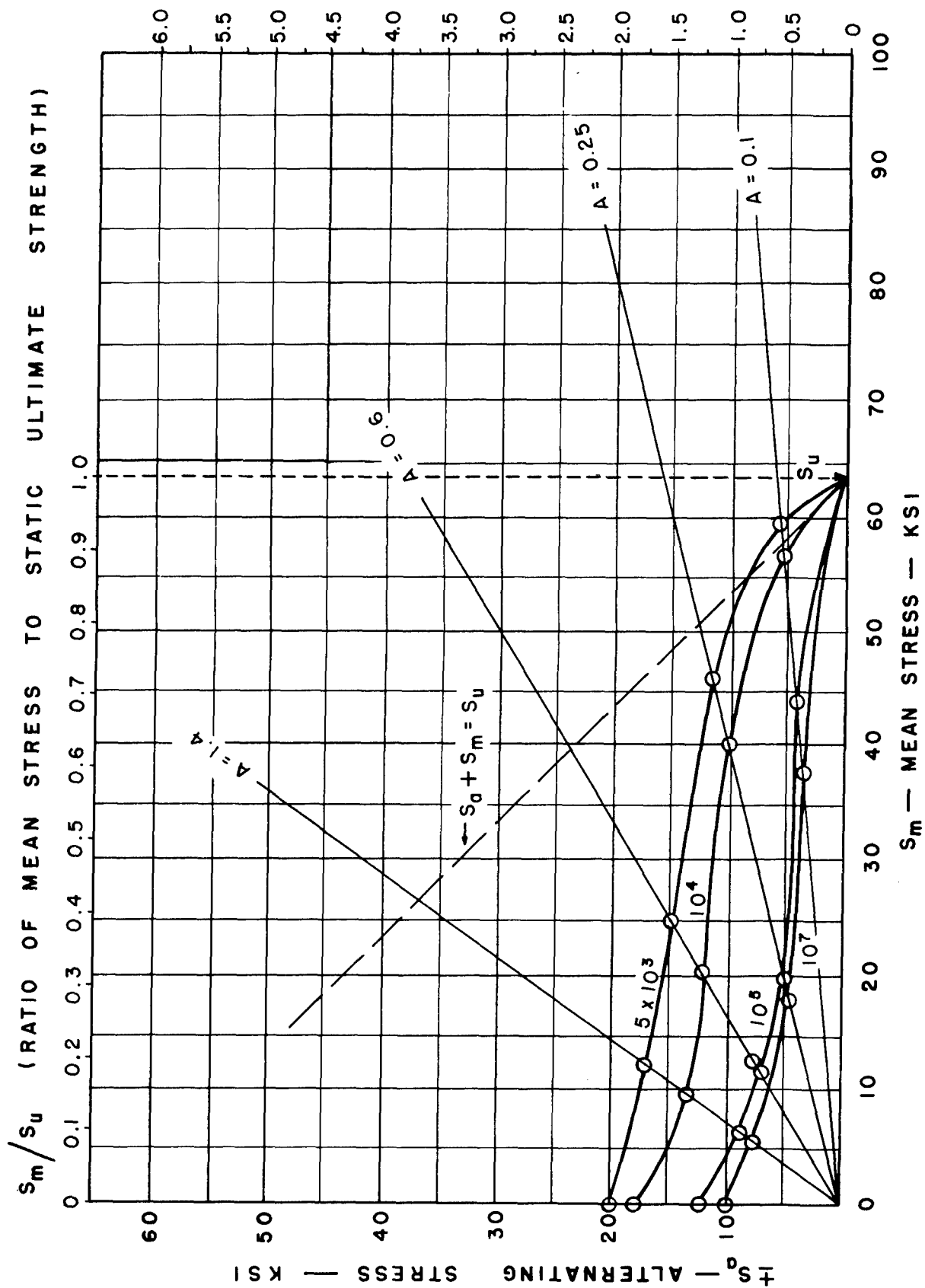


FIG. 7 STRESS-RANGE FATIGUE DIAGRAMS FOR  
TYPE AB SPECIMENS ( $K_t=2.4$ ) OF EXTRUDED MAGNESIUM ALLOY ZK60

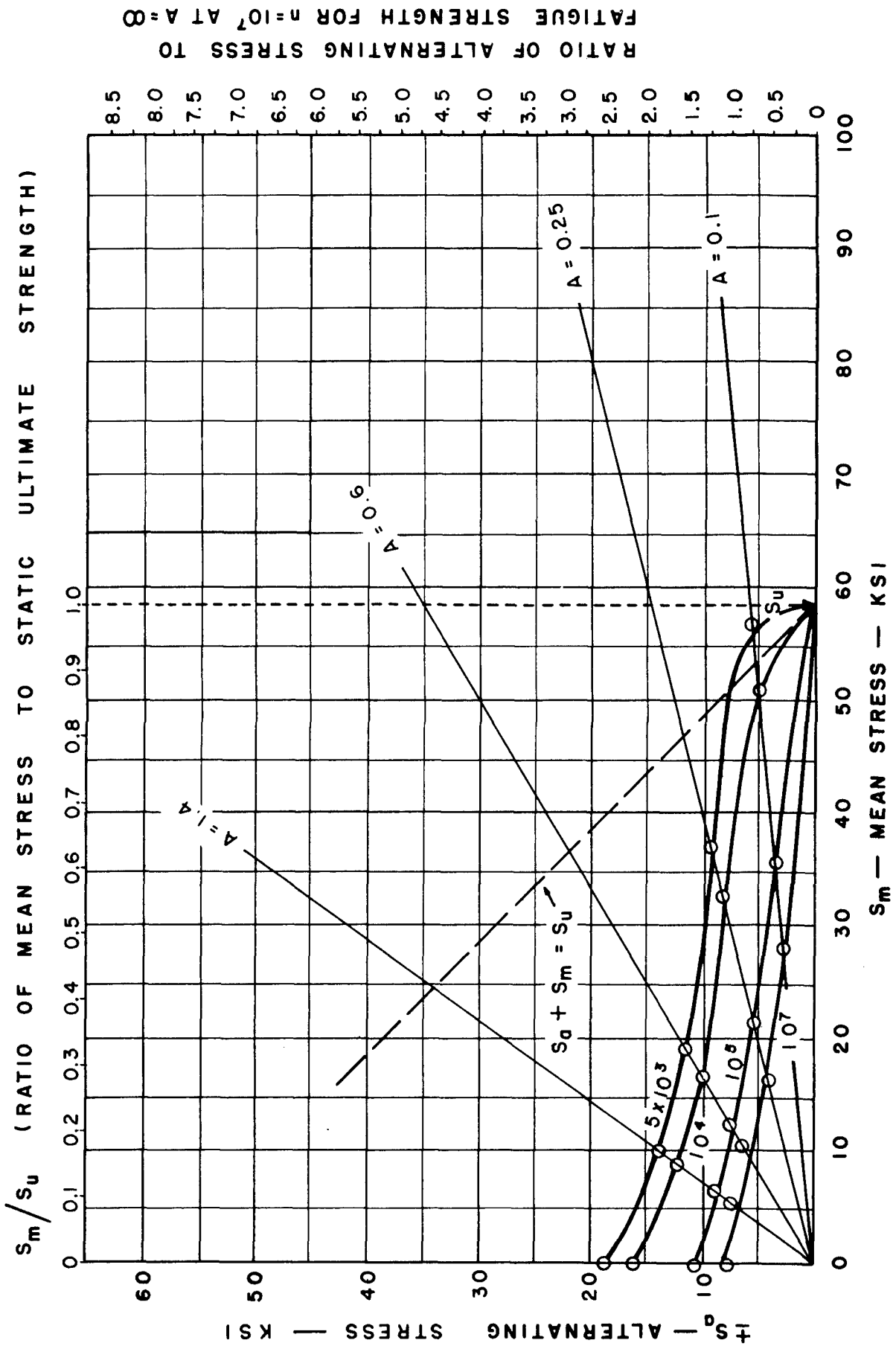


FIG. 8 STRESS-RANGE FATIGUE DIAGRAMS FOR  
TYPE X SPECIMENS ( $K_t=3.4$ ) OF EXTRUDED MAGNESIUM ALLOY ZK60

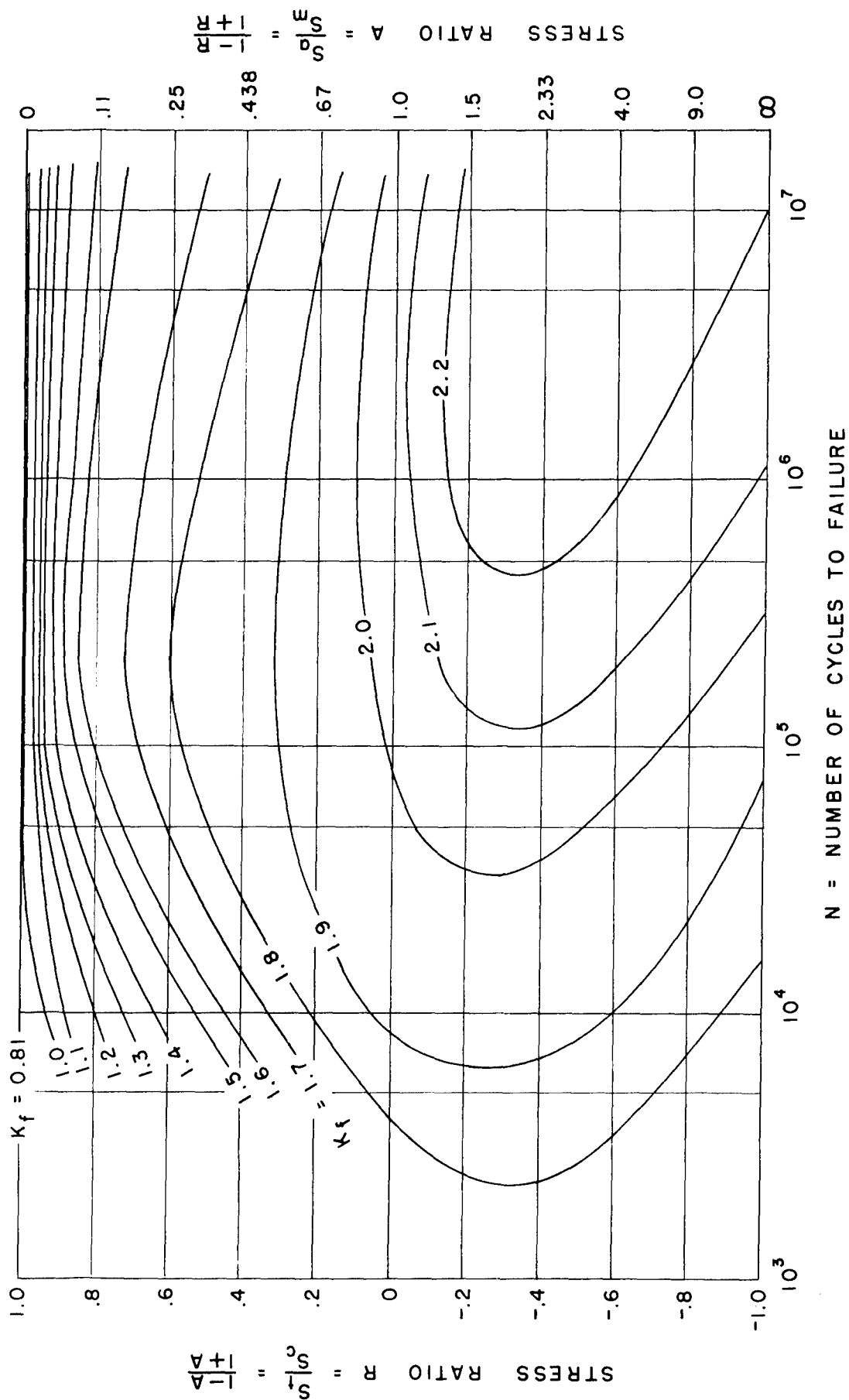


FIG. 9 FATIGUE STRENGTH - REDUCTION "CONTOUR" CURVES FOR  $K_f = 2.4$  SPECIMENS OF EXTRUDED MAGNESIUM ALLOY ZK60A-T5 SHOWING  $K_f$  AS A FUNCTION OF  $N$  AND STRESS RATIO



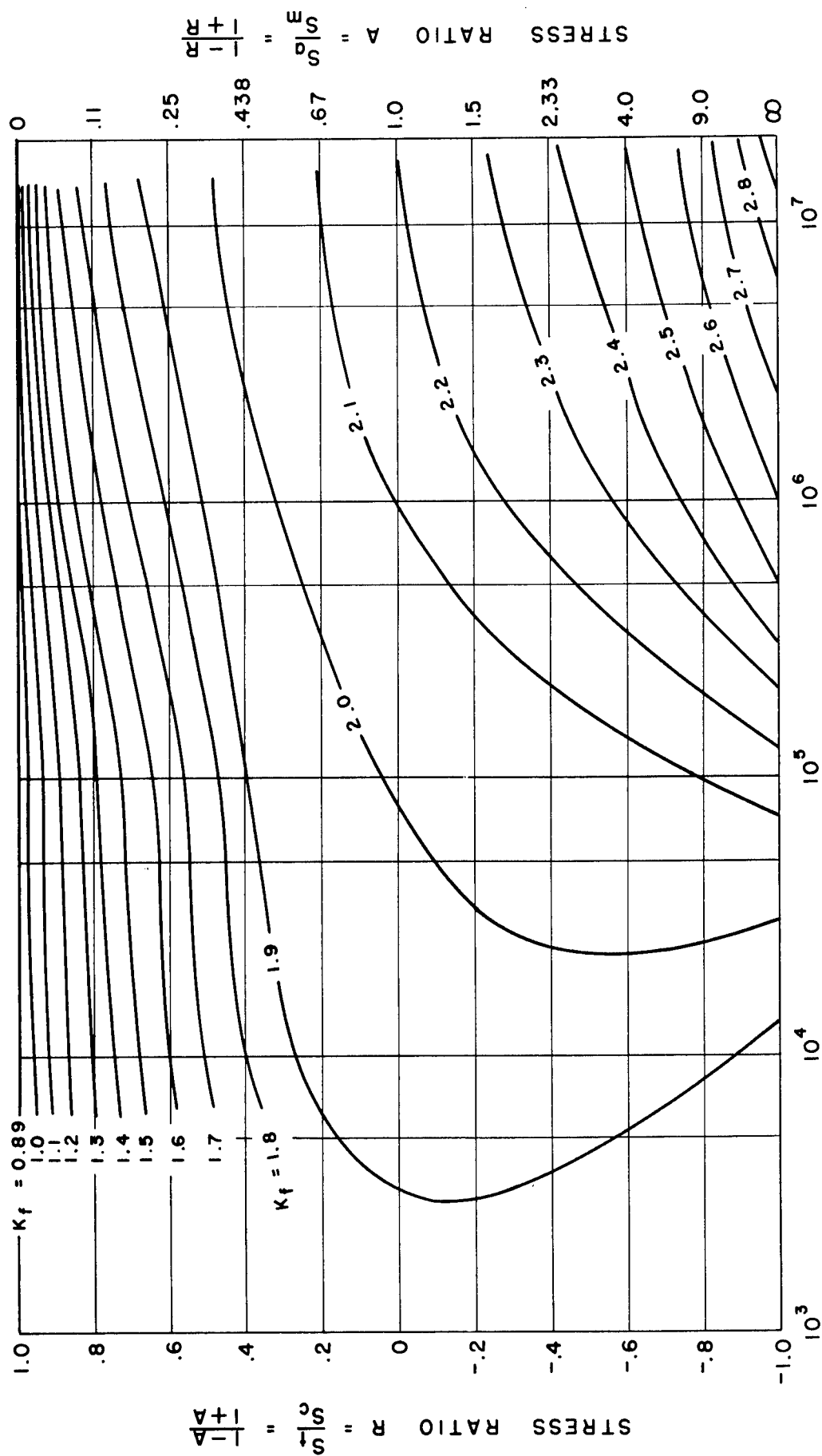


FIG. 10 FATIGUE STRENGTH - REDUCTION "CONTOUR" CURVES FOR  
 $K_t = 3.4$  SPECIMENS OF EXTRUDED MAGNESIUM ALLOY ZK60A-T5  
 SHOWING  $K_f$  AS A FUNCTION OF  $N$  AND STRESS RATIO

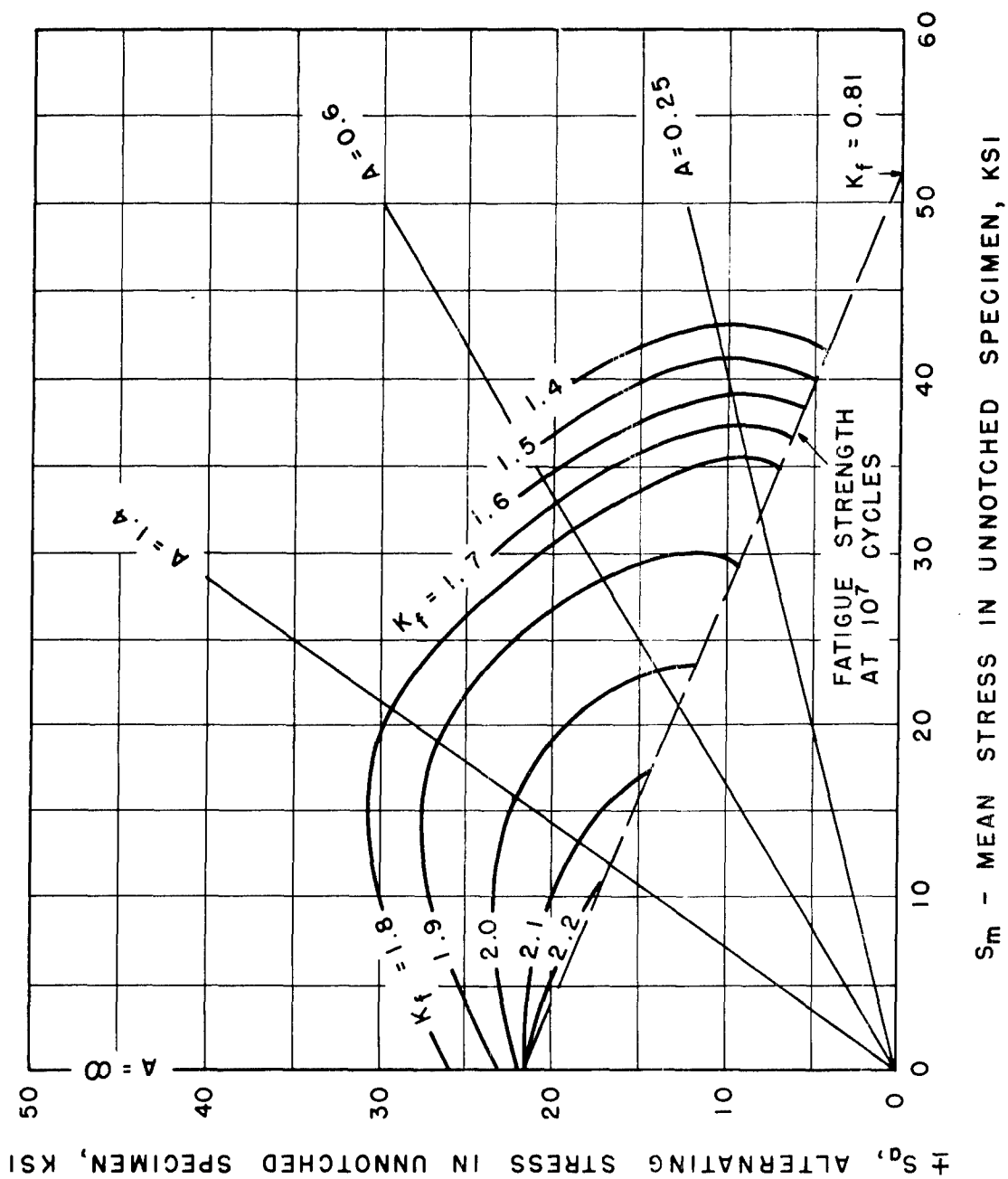


FIG. 11 FATIGUE STRENGTH - REDUCTION "CONTOUR" CURVES FOR  $K_t = 2.4$  SPECIMENS OF EXTRUDED MAGNESIUM ALLOY ZK60A-T5 SHOWING  $K_f$  AS A FUNCTION OF  $S_a$  AND  $S_m$  OF THE UNNOTCHED SPECIMENS

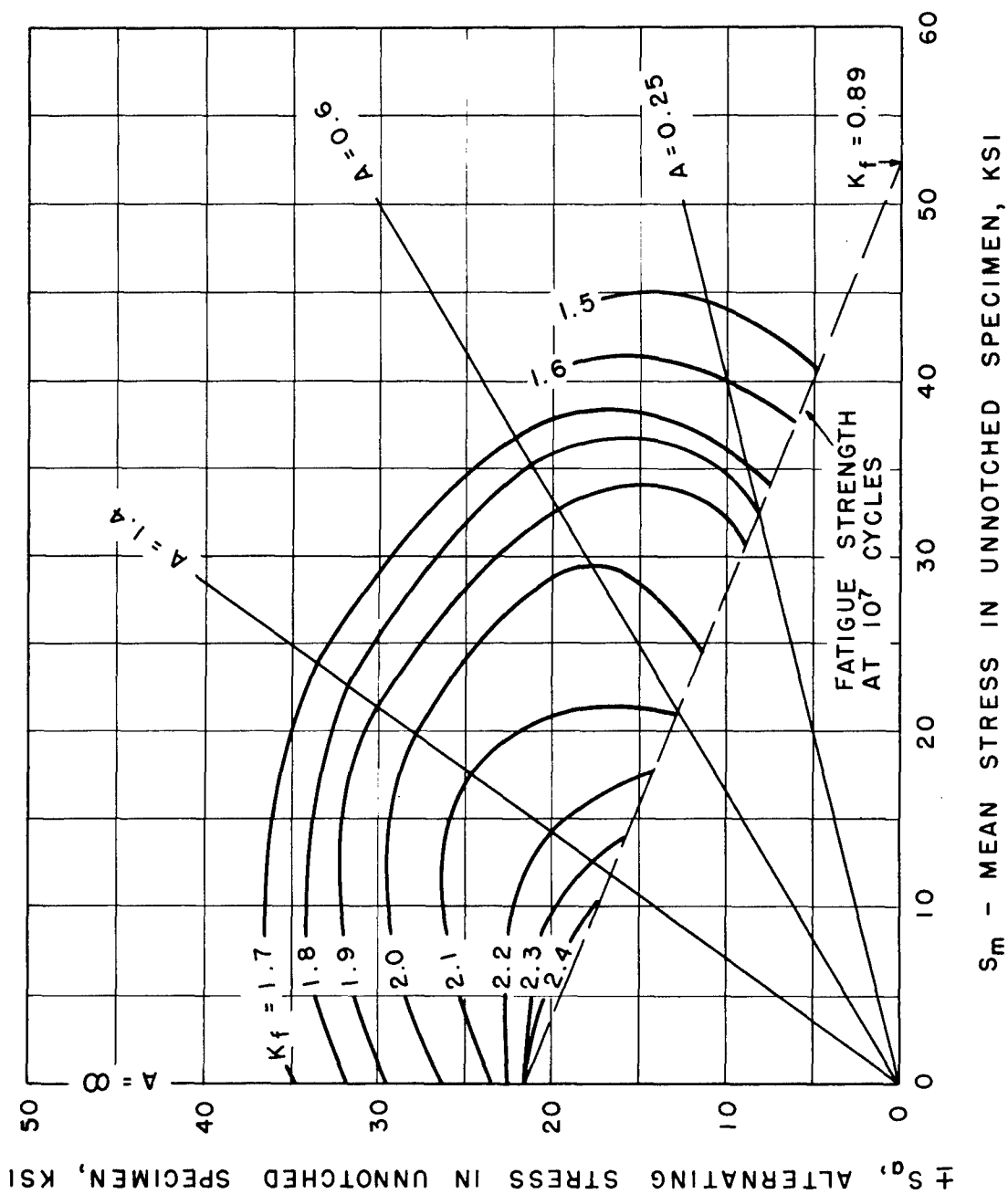


FIG. 12 FATIGUE STRENGTH - REDUCTION "CONTOUR" CURVES FOR  $K_t = 3.4$  SPECIMENS OF EXTRUDED MAGNESIUM ALLOY ZK60A-T5 SHOWING  $K_f$  AS A FUNCTION OF  $S_a$  AND  $S_m$  OF THE UNNOTCHED SPECIMENS